energy&fuels

pubs.acs.org/EF

Article

Ultrasound-Assisted Sequential Extraction for Lignocellulose Pyrolysis Bio-oil Fractionation. Part II: Comparative Application

Published as part of Energy & Fuels special issue "Celebrating Women in Energy Research".

Wladimir Ruiz, German Gascon, Ryan P. Rodgers, David C. Dayton, Caroline Barrère-Mangote, Pierre Giusti, Brice Bouyssiere,* and Martha L. Chacón-Patiño*

Cite This: *Energy Fuels* 2024, 38, 17697−17705

Read Online

ACCESS | Metrics & More | Article Recommendations | Supporting Information

ABSTRACT: Building upon the novel ultrasound-assisted sequential extraction (UASE) method introduced in Part I, the second paper delves deeper into the fractionation and analysis of bio-oils produced from lignocellulosic pyrolysis. The current study exploits advanced analytical techniques such as GPC-UV-DAD and negative-ion Electrospray Ionization (ESI) coupled with ultrahigh-resolution mass spectrometry, 21 T FT-ICR MS, to facilitate a detailed comparative analysis of various bio-oil samples produced from lignocellulosic pyrolysis. The results highlight significant differences in composition, molecular weight distribution, and oxygen content as a function of process conditions, which demonstrate the efficacy of the UASE method to distinguish different types of bio-oils. A sample generated by reactive catalytic fast pyrolysis (RCFP) reveals a composition that has potential for fuel production, evident by its low oxygen-to-carbon ratio and high concentration of non- to moderately polar fractions. Interestingly, the most polar fraction obtained by the UASE method has a GPC elution behavior consistent with lignin standards, indicating that the method unravels "undesired" pyrolysis byproducts and recalcitrant species. The characterization workflow presented confirms the potential of the RCFP process for fuel production and advances our understanding of bio-oil molecular composition. The insights gained are pivotal for advancing bio-oil processing techniques and standardizing quality assessment, especially for industrial applications, thereby continuing the advancement of bio-oil research established in the first paper of this two-part paper series.

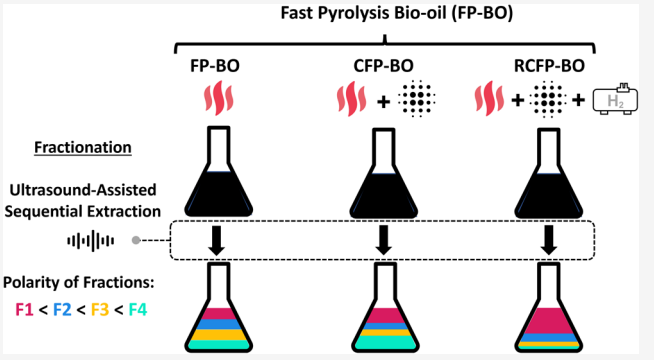

1. INTRODUCTION

The global shift toward sustainable energy solutions has brought lignocellulosic biomass into the spotlight as a viable alternative to fossil fuels. A significant development in this area is the transformation of this biomass into bio-oil, primarily through fast pyrolysis.[1] Unlike crude oil, pyrolysis bio-oils have a complex chemical composition rich in highly oxygenated molecules, due to abundant functional groups like alcohols, phenols, ethers, aldehydes, and acids. These functional groups are derived from the thermal decomposition of natural macromolecules like lignin, cellulose, and hemicellulose, making bio-oils highly complex and fundamentally different from fossil fuels in properties such as density, viscosity, solubility, and oxygen content.[2] Thus, their detailed characterization via diverse analytical methods is necessary to improve bio-oil processing.[3,4]

In complex mixture analysis (e.g., petroleum, asphaltenes, dissolved organic matter), fractionation plays a crucial role by dividing complex samples into simpler fractions for in-depth examination, enhancing understanding of their composition and properties.[5−9] In the case of pyrolysis bio-oils, the pioneering work of Oasmaa et al. since 1996 has guided the field.[10] The authors introduced the concepts of low molecular mass (LMM) and high molecular mass (HMM) lignin, which correspond to the soluble and insoluble fractions in dichloromethane (DCM).[11] This distinction led to the development of other liquid−liquid extraction methods,[12] which have led the investigation of bio-oil hydroprocessing performance.[13,14] Recent advancements in this field include the adoption of new liquid−liquid extraction techniques[11] and innovative methods like supercritical fluid extraction.[15] Traditional chromatographic techniques, which include silica-gel adsorption,[16] gel permeation chromatography (GPC),[17] flash

Received: May 26, 2024
Revised: July 24, 2024
Accepted: August 2, 2024
Published: August 19, 2024

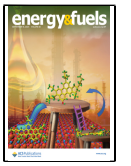

https://doi.org/10.1021/acs.energyfuels.4c02496
Energy Fuels 2024, 38, 17697−17705

chromatography,[18] centrifugal partition chromatography,[19] and sequential solubility extraction[20] have also been explored to enhance the analysis of bio-oils. The integration of these methods, from solvent extraction to chromatography, has streamlined the analysis process, enabling a more nuanced and detailed understanding of bio-oil composition.

The preceding manuscript, Part I of this series,[21] introduced the ultrasound-assisted sequential extraction (UASE) method using pure solvents for bio-oil fractionation. It focused on the fractionation of a fast pyrolysis bio-oil and its subsequent characterization by analytical techniques such as Gel Permeation Chromatography (GPC), Nuclear Magnetic Resonance (NMR), and Gas Chromatography−Mass Spectrometry (GCMS).[22−26] The findings revealed that the lighter fractions of bio-oil, F1 and F2, are rich in light aromatic compounds, making them suitable for hydrogenation into biofuels. Conversely, the heavier fractions, F3 and F4, have fewer aromatics and an increased content of sugar-like molecules, requiring a more effective, and likely not yet available, hydrogenation process. Notably, the GPC profile of F4 closely resembles that of lignin standards. Additionally, the average molecular weight of the fractions increased as a function of their polarity, which supported the findings of Van Aelst et al.[20]

GPC is a crucial tool in bio-oil research. It effectively compares bio-oil samples from different production processes, despite limitations in the identification of individual compounds. Such comparisons are crucial as they relate to the molecular characteristics that determine critical physical properties of bio-oils, such as density and viscosity.[27−29] Additionally, Fourier Transform Ion Cyclotron Resonance Mass Spectrometry (FT-ICR MS) offers significant insights at the molecular level, which enhances our understanding of bio-oil composition and aides in the study of processes like hydroprocessing through previously established methods in petroleomics.[30] Part II of this series aims to comprehensively evaluate the UASE method on four different pyrolysis bio-oils, derived from uncatalyzed, catalytic, and reactive catalytic processes. This evaluation focuses on molecular-level characterization and quality assessment. The extracted fractions and original bio-oils are analyzed using GPC-UV-DAD and negative-ion Electrospray Ionization (ESI) coupled with 21 T FT-ICR MS. The results demonstrate that the bio-oils derived from various processes exhibited a consistent trend across their fractions. The polarity, and thus, oxygen content of each fraction was proportional to its molecular weight. Moreover, molecular-level characterization revealed that the primary determinant of fractionation was the average oxygen-to-carbon (O/C) ratio within the fractions. While slight variations were noted among similar catalytic pyrolysis processes under different temperatures and feed rates, a significant difference emerged in the reactive catalytic fast pyrolysis process. This process yielded a significantly larger amount of the less polar, low molecular weight fraction, which exhibited a GPC profile consistent with its hydrotreated effluents.

2. MATERIALS AND METHODS

2.1. Samples. Four lignocellulose pyrolysis oils were fractionated by the UASE method developed in Part I of this study. The first bio-oil was produced by fast pyrolysis of pinewood and provided by BTG BTL (Enschede, Netherlands) company to TotalEnergies Research and Technology (Gonfreville, France); it is referred to as BO. The remaining three samples, each produced through different fast pyrolysis processes, were provided by the Research Triangle Institute, RTI International (North Carolina). Bio-oils referred to as CFP_1 and CFP_2, were produced from Douglas Fir crumbles using the same catalytic fast pyrolysis (CFP) process in a 1-ton-per-day (TPD) pilot plant, but under different operational conditions. CFP_1 was processed at a temperature of 480 °C and a feed rate of 57.7 kg/h. CFP_2 was produced in the same 1TPD pilot plant, but at a slightly lower temperature of 464 °C and a feed rate of 49.5 kg/h. Both samples utilized γ alumina as a catalyst. The sample labeled RCFP was produced by reactive catalytic fast pyrolysis (RCFP) of loblolly pine in a lab-scale fluidized bed reactor, 2.5 in. in diameter, under a hydrogen-rich atmosphere (80 vol %) and a MoO_3 catalyst on TiO_2 and ZrO_2 supports, at a mean temperature of 500 °C, fed at a rate of 4−5 g per minute.[31,32]

RTI International provided six effluents, labeled RCFP_1 to RCFP_6, which were recovered from the hydroprocessing of the RCFP sample. These effluents, essential for assessing the aging of the catalyst, were collected at intervals of approximately 36.5, 48.5, 72.5, 96.5, 124.5, and 143.5 h during a continuous hydrotreatment process. This process, which lasted 144 h, involved the treatment of the RCFP under a hydrogen pressure of 2000 psi in a pilot-scale hydroprocessing unit at RTI, with a total volume of 9.0 kg of bio-oil feed processed. The conditions maintained during the hydrotreatment included an average temperature of 300 °C in the reactor bed and a liquid hourly space velocity (LHSV) of 0.35/h, utilizing a sulfided hydrotreating catalyst. In a previous work, we analyzed the original RCFP sample and its hydrotreated effluents by 21 T FT-ICR MS. The results showed a notable change in composition, shifting from highly aromatic species with increased O/C ratios to molecules more suitable for biorefinery applications (lower oxygen, higher hydrogen contents).[30] In this study, however, we focus on their analysis by Gel Permeation Chromatography (GPC) with a UV Diode Array Detector (DAD), targeting their comparison with the original RCFP sample and its UASE fractions.

2.2. Solvents and Standards. HPLC-grade solvents were used for fractionation and various chromatographic analyses. *n*-Hexane, toluene, dichloromethane stabilized with 50 ppm amylene, and THF, both nonstabilized and stabilized with 250 ppm dibutylhydroxytoluene (BHT), were purchased from Scharlab, Spain. Alkali lignin or Kraft lignin (Sigma-Aldrich, Germany) was used as a standard to compare with the pyrolysis bio-oils. This standard is a conjugated base of lignin. A dispersion was formed by mixing 200 mg of alkali lignin in 3 mL of THF. Partial dissolution was achieved after adding two drops of concentrated HCl (Sigma-Aldrich, Germany). Following this, the THF-solubilized, regenerated lignin was separated from the resultant solids, alkaline chloride salts, and the excess of unreacted alkali lignin. This separation was achieved through filtration using a PTFE (polytetrafluoroethylene) filter with a 0.45 μm pore size purchased from VWR (Pennsylvania, USA).

2.3. Methodology and Instrumentation. *2.3.1. Bio-Oil Fractionation by Ultrasound Assisted Sequential Extraction.* The UASE fractionation method was performed on the four lignocellulose pyrolysis samples: BO, CFP_1, CFP_2, and RCFP. Approximately 1 g of the sample was placed in a 30 mL glass vial and mixed with 5 mL of *n*-hexane. Sonication was carried out using a BANDELIN electronic GmbH & Co. KG (Berlin, Germany) ultrasound device, operating at a frequency of 35 kHz and with a power of 40/160 W. Sonication was applied to the vial for 10 min at room temperature. The mixture was subsequently centrifuged at 1500 rpm for 5 min. The supernatant was collected in a preweighed vial. Extraction with *n*-hexane was repeated ten times. Subsequent extraction steps were carried out under the same conditions on the remaining insoluble bio-oil using toluene followed by dichloromethane. Each collected fraction, as well as the residual insoluble bio-oil was dried under N_2 until weight stabilization. The procedure yielded four fractions: hexane-soluble (F1), toluene-soluble (F2), dichloromethane-soluble (F3), and the residual bio-oil (F4). Each fraction was weighed to determine its mass percentage in the original sample and to assess the mass loss of volatiles and water in the drying process.

https://doi.org/10.1021/acs.energyfuels.4c02496
Energy Fuels 2024, 38, 17697−17705

The solvents hexane, toluene, and dichloromethane (DCM) were selected after initial solubility tests. Lignocellulose pyrolysis bio-oils have strong intermolecular interactions due to their high oxygen content. Nonpolar solvents like hexane and toluene are ineffective at breaking these interactions through simple stirring, whereas polar solvents (i.e., methanol) easily dissolve bio-oils. Ultrasound enhances dissolution by creating cavitation, partially disrupting the intermolecular interactions, and allowing each solvent to dissolve specific molecules. Preliminary tests indicated that the use of solvents under sonication resulted in a higher extraction of bio-oil. Thus, a sequential fractionation was developed to achieve selective separation, beginning with the least polar solvent and progressing to the solvent with the highest dipole moment. The UASE method was developed over a four-year period through rigorous testing of various approaches aimed at optimizing bio-oil fractionation. Multiple strategies, including liquid–liquid extraction, acid–base extraction, column chromatography, and extrography, encountered substantial challenges. For example, liquid–liquid extraction faced issues with solvent miscibility, leading to difficulties in biphasic separation. Acid–base extraction effectively separated phenolic compounds but resulted in significant mass losses during acid regeneration due to high solubility in water. Preparative column chromatography was deemed impractical due to uncontrolled elution from highly polar solvents required for sample loading. Therefore, UASE emerged as the most effective option. This process maintains sample integrity by circumventing interactions with solids and acid–base reactions. Notably, ten extraction iterations per solvent were executed to optimize UASE, with further extractions proving superfluous for yielding additional material.

2.3.2. Gel Permeation Chromatography (GPC). The GPC analyses were conducted using an UltiMate 3000 Dionex high-performance liquid chromatography (HPLC) system (Amsterdam, The Netherlands). This instrumentation included an UltiMate 3000 microflow pump, an autosampler, a low dead-volume port-to-port microinjection valve, and an ultraviolet diode array detector (UV DAD) set at 254 nm. The separation columns consisted of four styrene-divinylbenzene gel permeation columns, sourced from Waters Corporation (Milford, MA): HR4 (5 μm particle size; 600 000 Da polystyrene equivalent exclusion limit), HR2 (5 μm particle size; 20 000 Da exclusion limit), and two HR0.5 columns (5 μm particle size; 1000 Da exclusion limit). Additionally, a Styragel guard column (4.6 mm i.d. × 30 mm) was incorporated to extend the operational lifetime of the series columns. For analyses, bio-oil samples and fractions were diluted (100-fold by weight) in stabilized THF. Chromatographic runs involved an isocratic elution of a 20 μL sample solution with THF at a flow rate of 0.8 mL/min over 65 min. The system was calibrated with polystyrene (PS) standards with molecular weights from 162 to 3152 Da. This calibration established a polynomial relationship linking molecular weight (MW), expressed as equivalent polystyrene, and chromatographic retention time (t), as shown in eq 1 (the calibration curve is included in in Figure S1). Python notebooks assisted data visualization.

$$\log(\mathrm{MW}) = -1.22 \times 10^{-4} t^3 + 1.90 \times 10^{-2} t^2 - 1.05t + 22.1 \quad (1)$$

2.3.3. Negative-Ion ESI Coupled to 21 T FT-ICR MS. For negative-ion electrospray ionization (−ESI), samples were diluted in methanol to a concentration of 25 μg/mL. Samples were directly infused at 0.55 μL/min and ionized with a needle voltage of −3.4 kV. Ions were analyzed with a custom-built 21 T FT-ICR mass spectrometer.[33,34] In this process, 2×10^6 charges were accumulated for 1−3 ms in an external multipole ion trap, with the accumulation period determined by automatic gain control (AGC). Ions were transferred to the ICR cell, as a function of m/z and subsequently excited, maximizing the number of detected peaks. Excitation and detection were achieved on the same pair of electrodes, with the ICR cell operated at 6 V. Time-domain transients of 3.2 s were collected with Predator Software, and 150 transients were averaged for each sample. Mass spectra were phase-corrected and internally calibrated with at least a hundred oxygen-containing molecular formulas using "walking" calibration. PetroOrg software assisted molecular formula assignment and data visualization in van Krevelen diagrams and DBE vs carbon number plots. The ultrahigh mass accuracy and resolving power of the 21T FT-ICR mass spectrometer yield remarkable assignment performance for complex mixtures. In this study, most of the assigned compositions feature errors below 0.2 ppm. Only compound classes with a relative abundance of ≥0.10% were considered for data interpretation. Raw mass spectra, calibrated peak lists, and PetroOrg files are publicly available at Open Science Framework, DOI 10.17605/OSF.IO/JRVQG. Van Krevelen plots were generated for selected oxygen classes, specifically O_5 to O_{28}. The O_1 to O_4 classes were excluded due to the presence of prominent "contaminant" peaks, such as fatty acids commonly observed as background ions in negative-ion ESI.

3. RESULTS AND DISCUSSION

3.1. Gravimetric Analysis of Samples. Figure 1 illustrates the mass percentage distribution of the four

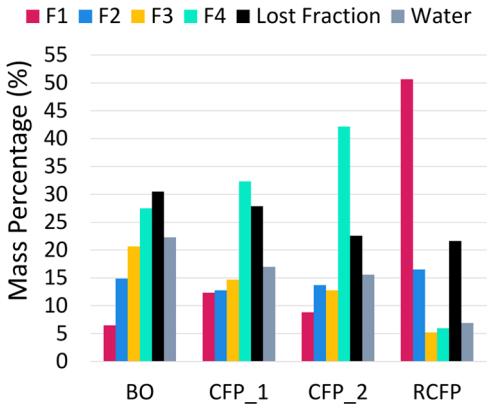

Figure 1. Mass percentage for the bio-oil fractions for BO, CFP_1, CFP_2, and RCFP samples. Black bars represent the mass percentage for the lost fraction during the fractionation and drying process due to volatilization. The original water content determined by Karl Fisher is highlighted in gray.[18,31,32,35]

recovered fractions (F1, F2, F3, and F4) and the lost material (black bars) fraction across various bio-oil samples, i.e., BO, CFP_1, CFP_2, and RCFP. Detailed information on these samples is included in Table S1. Table S2 of the Supporting Information shows the repeatability of the fractionation method for the BO sample. In this case, the relative standard deviation (RSD) is consistently below 6%. The water contents of the whole samples, determined using the Karl Fischer method, were previously published as 22% for BO, 17% for CFP_1, 16% for CFP_2, and 7% for RCFP. These values are shown as gray bars in Figure 1.[18,31,32,35] The results indicate that under catalytic conditions, the water content in the bio-oil is reduced. When we consider that the water represented by the gray bars evaporates during the drying process, it becomes clear that the lost fraction, indicated by the black bars, includes more than just water. We hypothesize that this fraction mainly consists of light molecules such as methanol, acetic acid, acetol, and some light aromatics, as explained in Part I of this study.[21] Moreover, the RCFP oil sample exhibits a higher concentration of these light, nonaqueous molecules, which are lost during the fractionation process and are likely byproducts of hydrocracking reactions that occurred during pyrolysis.

In Part I of this study,[21] we observed a gradual increase in the polarity of the UASE bio-oil fractions. This trend aligns with the increasing polarity of the solvents used in each successive UASE extraction step. With the simple fast pyrolysis bio-oil (BO), there was a gradual increase in mass percentage

https://doi.org/10.1021/acs.energyfuels.4c02496
Energy Fuels 2024, 38, 17697−17705

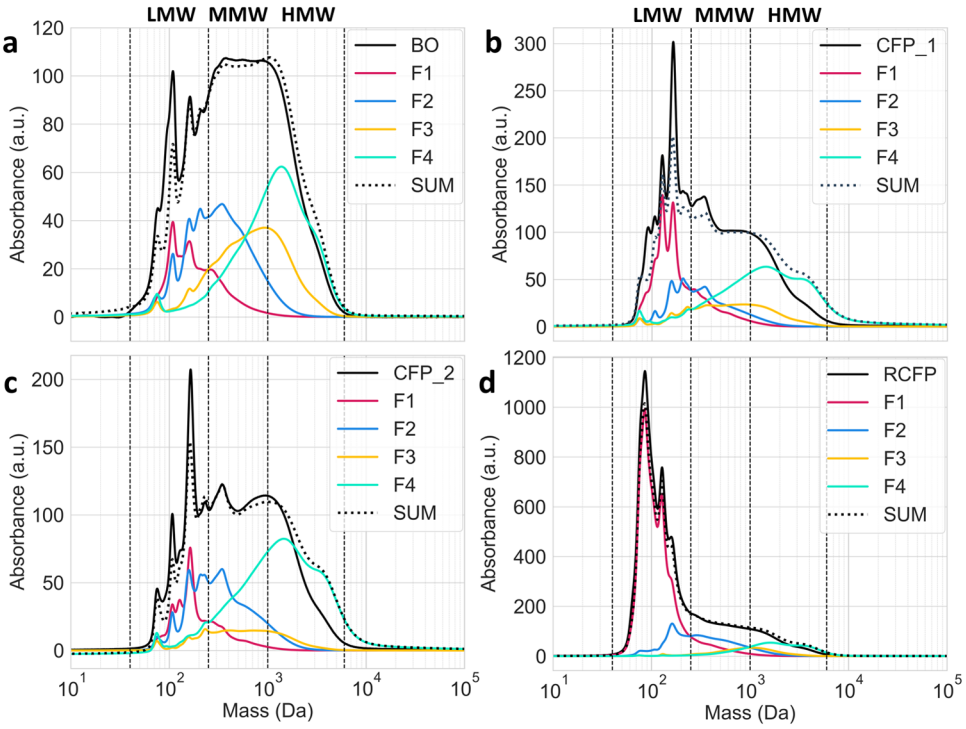

Figure 2. GPC-UV-DAD chromatograms of whole bio-oil samples: (a) BO, (b) CFP_1, (c) CFP_2, and (d) RCFP, with fractions (F1, F2, F3, and F4) corrected with their respective gravimetric factors, and reconstructed chromatogram obtained from the sum of the corrected signals (SUM) at 254 nm.

from F1 to F2, and similarly from F2 to F3, and F3 to F4. In contrast, the catalytic fast pyrolysis bio-oils (CFP_1 and CFP_2) did not exhibit this trend. Although the nature of the process was fundamentally the same for both catalytic samples, the operational conditions, such as temperature and feed rate, differed. CFP_1 operated at higher values (480 °C and 57.7 kg/h) compared to CFP_2 (464 °C and 49.5 kg/h). A key observation was that CFP_2 had the highest content (42.2%) of the most polar fraction (F4) and the lowest content of F1 (8.8%), whereas CFP_1 contained 12.3% of F1. This suggests that the lower temperature and feed rate in CFP_2 may not favor optimal conversion of high-molecular-weight biomass molecules. Figure 1 illustrates that the reactive catalytic process (RCFP) yielded a bio-oil with significantly higher content of nonpolar products, accounting for 50.7% of F1, which is substantially greater than the other samples, all of which contain less than 13% of F1. For RCFP, combined F1 and F2 fractions constitute nearly 70% of the total sample, whereas F3 and F4 are present in much smaller proportions, only up to 11.2%.

Based on the results reported in Part I of this study,[21] the gravimetric data alone reveals significant chemical differences between the bio-oils, even without the need for instrumental analysis. For instance, RCFP stands out as the most promising bio-oil for fuel applications. Furthermore, the data suggests that the catalytic processes used in CFP_1 and CFP_2 may not offer significant advantages when compared to the noncatalytic process used for BO. It is important to highlight that under ultrasonic conditions, hexane effectively extracted most light aromatics, such as guaiacol derivative molecules, as previously confirmed by GC-MS.[21] On the other hand, carbohydrate-like compounds predominantly remained in the more polar fractions.

3.2. Gel Permeation Chromatography Analysis.

The samples were analyzed by GPC to evaluate the differences in hydrodynamic volume and estimated molecular weight between the original bio-oils and their fractions. A UV-DAD detector set at 254 nm was used, as most samples contain aromatic molecules. In GPC, the weight fraction (w_i) of each polymer chain is determined by measuring their absorbance (A_i) (see eq 2a). This reveals the proportion of different polymers in the sample. Two types of average molecular weights are then calculated. The number-average molecular weight (M_n) uses w_i and reflects the average based on the frequency of each polymer chain's molecular weight (M_i) (see eq 2b). The weight-average molecular weight (M_w) gives more importance to larger polymer chains due to their greater mass (see eq 2).

$$\text{(a) } w_i = \frac{A_i}{\sum A_i} \quad \text{(b) } M_n = \frac{\sum (w_i \cdot M_i)}{\sum w_i}$$
$$\text{(c) } M_w = \frac{\sum (w_i \cdot M_i^2)}{\sum (w_i \cdot M_i)} \tag{2}$$

Figure 2 features the GPC chromatograms of the four bio-oil samples: BO, CFP_1, CFP_2, and RCFP. Each data set is presented with corrections applied to the respective fractions using gravimetric factors and reconstruction (SUM). The molecular weight regions, as defined in Part I of this study, are low molecular weight (LMW) from 40 to 250 Da, medium molecular weight (MMW) from 250 to 1000 Da, and high molecular weight (HMW) from 1000 to 6000 Da, marked by vertical dashed lines in the chromatograms. The results indicate that for all bio-oil samples, their fractions revealed an increase in molecular weight as a function of polarity

https://doi.org/10.1021/acs.energyfuels.4c02496
Energy Fuels 2024, 38, 17697−17705

increase, which is supported by the M_n and M_w values in Table S3.

The chosen wavelength is representative of bio-oils for qualitative analyses.[28] The molar absorptivity of molecules may vary depending on their functional groups and molecular size. GPC chromatograms, set at 254 nm, are used as a comparative tool to assess fraction differences. Even though there are variations in absolute intensity due to different molecular structures, the similarity between the reconstructed GPC profile and that of the original samples confirms the reliability of the UASE method. In addition, previous research by Harman-Ware et al.[27,28] has demonstrated that consistent and comparable results can be obtained when analyzing similar lignocellulose pyrolysis bio-oil samples using GPC-UV (280 nm), GPC-RI, and GPC-MALS.

Furthermore, Figure 2 indicates that each bio-oil features a unique GPC profile. The reconstructed chromatograms (SUM) of all bio-oils closely resemble those of the original samples, despite mass losses during fractionation and drying processes. We hypothesize that the reason for this similarity is that the mass losses, primarily water and volatile molecules like methanol and acetic acid, cannot be detected by UV−vis (Supporting Information, Figure S2). As a result, these substances do not affect the GPC chromatograms of whole bio-oil samples. Conversely, the recovered fractions are mainly composed of highly aromatic molecules that are detectable by UV−vis. However, for the CFP_1 and CFP_2 samples, aromatic species in the most polar fraction (F4) seem more prevalent than in the unfractionated sample. This result indicates possible aggregation or polymerization during or after fractionation, which is likely influenced by changes in supramolecular interactions. In the original bio-oil sample, the complex mixture's constituents interact differently than when the most polar molecules, as in fraction F4, are isolated.

The RCFP sample features a high proportion of the less polar fraction (shown by gravimetric analysis), which is reflected in its GPC chromatogram, with most of the sample falling within the LMW region. These findings, especially regarding the RCFP sample, are important for fuel production as it is shown that the reactive catalytic process yields a bio-oil abundant in species with lower polarity and molecular weight, which is desirable for fuel applications.

The direct comparison of the size distributions of various bio-oils (BO, CFP_1, CFP_2, and RCFP) in their original form is quite complex (see Figure 2). To facilitate a clearer comparison, fractions F1 to F4 were normalized and individually analyzed in Figure 3. F1, characterized by lower polarity, predominantly appears in the LMW region, with a minor presence in the MMW region. The relative intensity in the MMW region is more pronounced for BO compared to CFP_1 and CFP_2. Notably, RCFP exhibits an almost exclusive presence in the LMW region, and features a minimal signal intensity in the MMW region. In fractions F1, the different chromatographic profiles across the various bio-oil samples could suggest the selective production of specific pyrolysis monomers with different retention times or sizes, as clearly shown in Figure 3a.

Regarding the F2 fractions, all bio-oils have a distribution that covers both the low and medium molecular weight (LMW and MMW) regions, with a minor presence in the high molecular weight (HMW) range, as shown in Figure 3b. As for F3 fractions, the LMW population decreases, and the majority of the compositions are present in the MMW and HMW

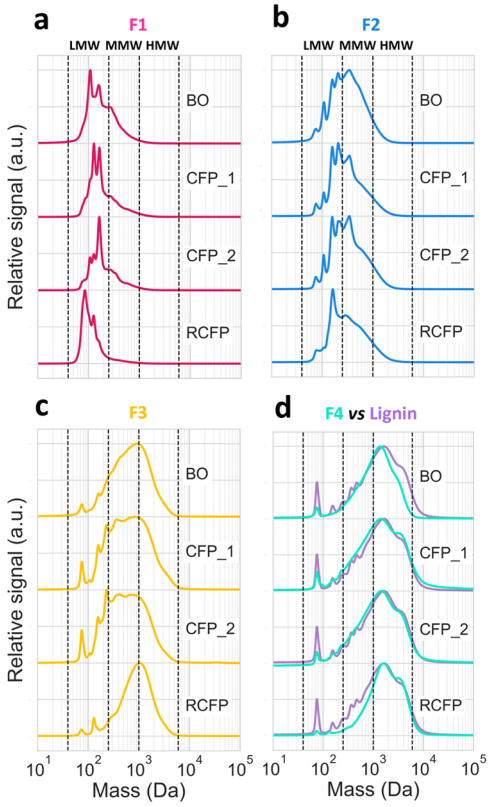

Figure 3. GPC-UV-DAD chromatograms with normalized intensity for fractions (a) F1, (b) F2, (c) F3, and (d) F4, for the different bio-oil samples (BO, CFP_1, CFP_2, and RCFP). Data for the regenerated alkali lignin, at 254 nm, is shown in panel d.

regions. Interestingly, the F3 fraction of RCFP has a notably lower population in the LMW and MMW regions, which likely suggests a more selective separation for the RCFP sample (Figure 3c). Finally, F4 fractions predominantly reside in the HMW region, with decreasing populations in MMW and minimal presence in LMW (Figure 3d). Across all bio-oils, F4 displays a size distribution similar to that of the regenerated alkali lignin standard (highlighted in purple in Figure 3d). This implies that F4 is the most polar and refractory fraction of the bio-oil samples, and therefore, such species should be hydroprocessed with advanced upgrading methods. The observed peak in the lignin standard below 100 Da likely corresponds to low molecular weight compounds. These compounds may be degradation products resulting from the alkaline treatment used in the extraction of lignin from natural sources.

Based on the analysis of various bio-oils, RCFP emerges as a potentially optimal candidate for hydroprocessing due to its higher concentration of LMW compounds. In hydroprocessing treatment conducted on RCFP, various effluents (RCFP_1 to RCFP_6) were collected at different time on stream (TOS) and analyzed using GPC for comparison with fractions derived from the UASE method (data presented in Figure 4). A key observation from the analysis of RCFP hydroprocessing effluents is that nearly 100% of the compounds are located in the LMW region (Figure 4a). Additionally, a decrease in relative absorbance is noted, which is consistent with an expected reduction in aromaticity compared to that of the original feed. Indeed, the effluents RCFP 1 and 2 have been previously analyzed by ultrahigh-resolution mass spectrome-

https://doi.org/10.1021/acs.energyfuels.4c02496
Energy Fuels 2024, 38, 17697−17705

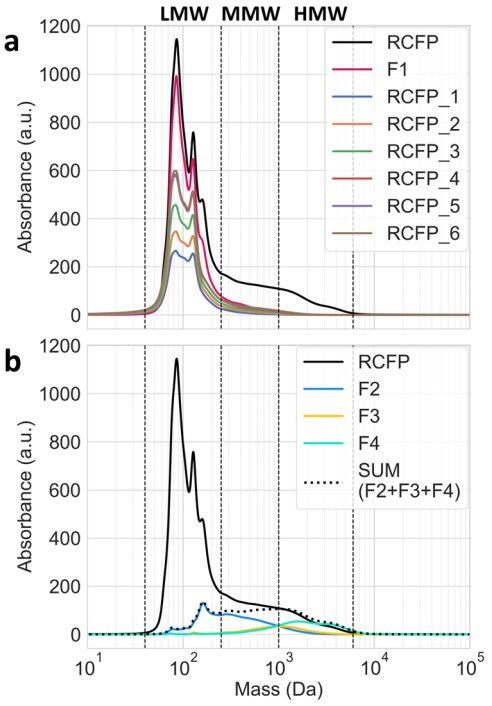

Figure 4. GPC-UV-DAD chromatograms for (a) the RCFP sample, its F1 fraction, and whole hydrotreated effluents collected at different TOS during continuous hydroprocessing (RCFP_1 at 36.5 h, RCFP_2 at 48.5 h, RCFP_3 at 72.5 h, RCFP_4 at 96.5 h, RCFP_5 at 124.5 h, and RCFP_6 at 143.5 h); and (b) the RCFP sample and its F2, F3, and F4 fractions along with the reconstruction (SUM) at 254 nm.

try,[30] and the observed compositional trends indicated that these effluents featured the lowest aromaticity and O/C ratios. Furthermore, they also pointed to possible catalyst deactivation starting from the time-point in which RCFP_3 was collected.

In this work, from the start of the process up to 96.5 h (RCFP_4, Figure 4a), there is a consistent increase in the absorbance of the effluents, which suggests a rise in aromaticity. This trend may indicate a gradual deactivation of the catalyst during the hydrogenation process. Beyond this point, the absorbance remains consistent up to the collection of the final effluent at 143.5 h. An interesting finding is the similarity of molecular weight between fraction F1 of the RCFP sample prior to hydrotreatment, and the whole hydroprocessed effluents (RCFP_1−6). Conversely, the more polar fractions, F2, F3, and F4 (data included in Figure 4b), are not present after hydrogenation. These observations hold significant potential for tracking and optimizing catalytic processes. For instance, despite the apparent catalyst deactivation over time, the more polar fractions remain undetectable in the hydrotreated effluents. If the catalyst deactivation is caused by highly polar fractions, their specific effects could be better understood by conducting hydroprocessing on isolated fractions in a controlled laboratory setting. A detailed examination of how specific compound families interact with the catalyst would significantly contribute to optimizing hydroprocessing methods.

3.3. Negative-Ion ESI Coupled to 21 T FT-ICR MS. FT-ICR MS was used to access thousands of molecular formulas in each of the bio-oil fractions. Figure 5a presents the compositional range, i.e., van Krevelen diagrams, for the whole samples and the respective fractions. These graphs feature the molecular formulas in terms of H/C and O/C ratios, and they are valuable tools for evaluating the energy density of bio-oil molecules. The color scale is the relative abundance normalized within each sample. Molecules ideal for biorefinery purposes have high H/C and low O/C ratios, and fall within zone 1, defined by $1.5 \leq H/C < 2$ and $0 < O/C \leq 0.3$. In contrast, less desirable molecules feature $0.5 < H/C < 1.5$ and $0 < O/C < 0.67$, placing them in zone 2, which is consistent with biochar composition.[36] Additionally, molecules with $1.5 < H/C < 2$ and $O/C > 0.3$ are similar to lignin or biomass species and belong to zone 3.[30]

Figure 5a,b show the shift in composition, from a noncatalytic process (BO) to reactive catalytic upgrading (RCFP), indicating a decrease in the average O/C values: 0.41 for BO, 0.28 for CFP_1, 0.33 for CFP_2, and 0.20 for RCFP. These data confirm that van Krevelen diagrams can effectively illustrate deoxygenation by highlighting the loss of oxygen in specific atomic ratios, such as dehydrogenation, which precisely shifts molecules in zone 3 of the van Krevelen diagram to the bottom left corner in zone 2. The results indicate that F1 and F2 fractions comprise abundant compositions with O/C ratios <0.4. As the separation advances, the distribution of species broadens, and F3 and F4 fractions feature higher O/C (>0.4) and H/C (>1.3) ratios, with elemental compositions that are consistent with carbohydrate-like compounds and decomposition products from cellulose, lignin, and hemicellulose. Indeed, Figure 5b indicates that the abundance-weighted O/C ratios increase as a function of increasing fraction number.

Thus, the data reveals that the most polar fractions contain larger, incompletely pyrolyzed biomass oligomers, which is highlighted in the van Krevelen diagrams by a pink dashed line. These species have more oxygen atoms in their structures compared to the monomers detected in less polar fractions. This fact is supported by Figure 5c, which features the compound class distribution for the CFP_2 whole sample and derived fractions. The data for the rest of the bio-oils are included in Figure S3. Figure 5c indicates that the F1 fraction has abundant molecules with less than seven oxygen atoms, with an abundance-weighted O/C ratio of 0.22 (highlighted in red in the respective van Krevelen diagram). Conversely, the F4 fraction features abundant species with higher oxygen numbers (e.g., O_{10}-O_{28}) and an abundance-weighted O/C = 0.43. It is important to emphasize that separation of bio-oil into fractions improves MS performance for complex mixture applications. Fractionation reduces signal suppression, which commonly occurs when analyzing complex, polar (heteroatom rich) samples.[6,8,37,38] As a result, each fraction represents a less complex matrix, allowing access to a wider range of compositions. The Supporting Information, Figure S4, features the combined Van Krevelen plots for all the fractions for each bio-oil sample, and clearly shows that the molecular-level information obtained from fraction analysis is more comprehensive than that from direct infusion MS of whole samples.

Collectively, the results highlight that the whole RCFP bio-oil is the sample with the lowest O/C ratios. This is consistent with RCFP's UASE fraction distribution, as it features the highest amount of F1. The data also indicates that BO contains species with the highest O/C ratios; higher than the catalyzed fast pyrolysis oils, CFP_1 and CFP_2. This suggests that the proposed fractionation and GPC methodology, supported by

https://doi.org/10.1021/acs.energyfuels.4c02496
Energy Fuels 2024, 38, 17697−17705

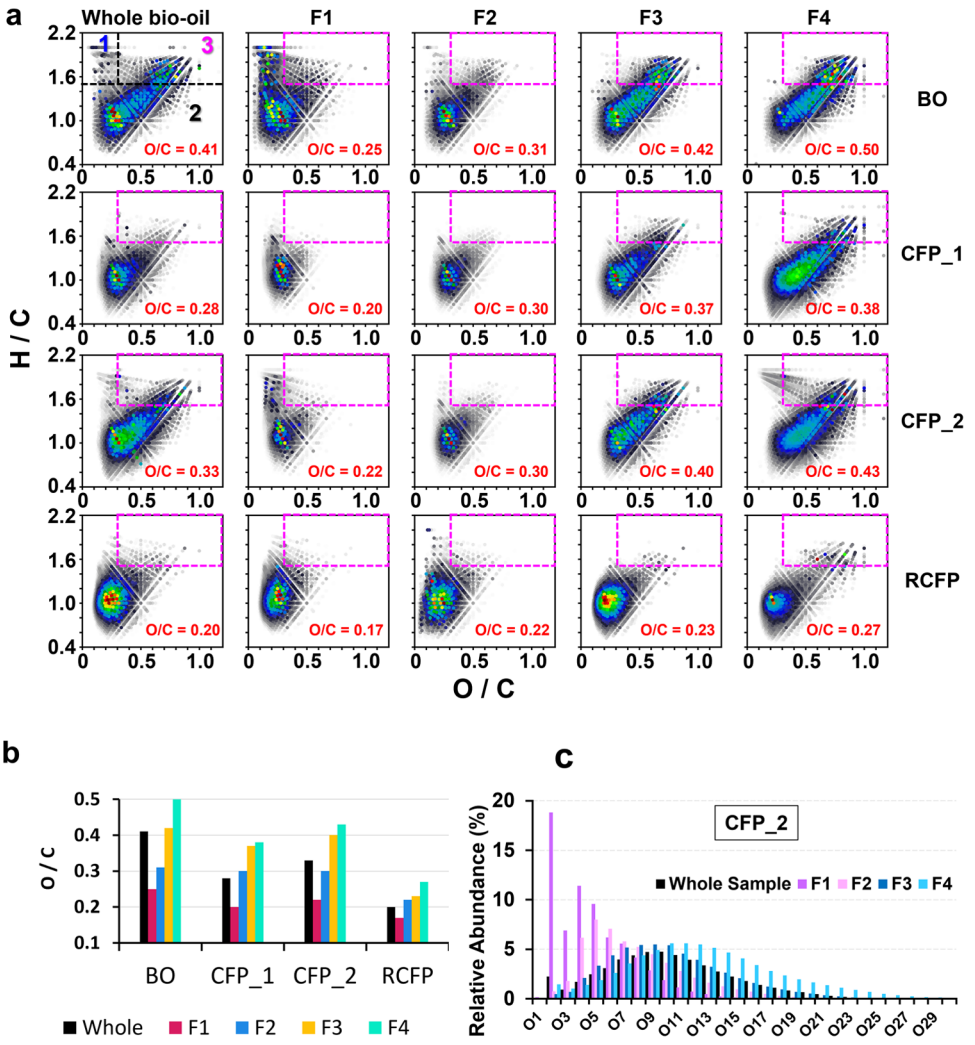

Figure 5. (a) Van Krevelen Plots for combined O_x classes (O_5−O_{28}) for whole bio-oil samples and their UASE fractions; (b) abundance weighted O/C ratios derived from −ESI FT-ICR MS data; and (c) heteroatom class distribution for CFP_2 whole sample and derived fractions. Abundance-weighted O/C ratios for all samples are included in red within the van Krevelen diagrams. The plot in the upper-left corner highlights zones 1, 2, and 3.

FT-ICR MS data, can eventually be used to evaluate process performance and trace the effect of catalyst use.

4. CONCLUSIONS

This study provides a comparative analysis of bio-oil samples (BO, CFP_1, CFP_2, and RCFP), employing the UASE fractionation process and analytical methods such as GPC-UV-DAD and negative-ion ESI coupled to 21 T FT-ICR MS. These methods have revealed significant variations in composition, molecular weight distribution, and oxygen content, which highlight the effectiveness of UASE fractionation. The gravimetric analysis indicates that the RCFP sample features the highest proportion of the less polar fraction, F1, which suggests the prevalence of hydrogen-rich species with properties desirable for biofuel applications. GPC analysis correlates the polarity of the fractions with their average molecular weight, which shows consistency across all samples. The most polar fraction, F4, aligns with the GPC elution profile of the regenerated lignin standard. Therefore, the results suggest that F4 compounds are likely undesired byproducts from pyrolysis processes or incompletely reacted biomass polymers. FT-ICR MS analysis deepens the understanding of the molecular composition of the samples, notably linking fraction molecular weight/size, polarity, and oxygen content. The lower O/C ratio for the RCFP sample points to its suitability for fuel applications.

Regarding RCFP hydroprocessing, GPC and UASE fractionation revealed that the most polar fractions (F2, F3, and F4) likely undergo complete cracking, deoxygenation, and hydrogenation, and the species detected in the LMW range (effluents RCFP_1 to RCFP6) resemble those of the F1 RCFP fraction. Cracking and hydrogenation persist even with reduced catalyst efficiency, which we hypothesize is a key insight for optimizing hydroprocessing. In summary, this work emphasizes RCFP as the preferred option for biofuel production, with CFP_1 and CFP_2 showing little advantage over uncatalyzed processes (BO). More notable differences between BO and CFP bio-oils were evident in the mass spectral data included in Figure S3. This knowledge is crucial for bio-oil production and upgrading, particularly for industrial applications.

https://doi.org/10.1021/acs.energyfuels.4c02496
Energy Fuels 2024, 38, 17697−17705

■ ASSOCIATED CONTENT

Supporting Information

The Supporting Information is available free of charge at https://pubs.acs.org/doi/10.1021/acs.energyfuels.4c02496.

Calibration curve of polystyrene standards in the GPC columns (Figure S1); Mass percentage distribution of bio-oil samples (BO, CFP_1, CFP_2, and RCFP) across fractions F1, F2, F3, and F4, as well as the mass lost during the fractionation process due to volatilization (Table S1); Mass percentage values for fractions F1, F2, F3, F4, and overall recovery in three fractionation replicates of BO fast pyrolysis oil, along with their calculated mean, standard deviation (SD), and coefficient of variation (CV) (Table S2); GCMS analysis of light volatiles potentially lost during the solvent evaporation process of the UASE method (1, Methanol; 2, Acetic acid; 3, Acetol; 4, Guaiacol; 5, Creosol) (Figure S2); Number-average (M_n) and weight-average (M_w) molecular weights (in Daltons) and polydispersity index (M_w/M_n) derived from GPC data for various fractions of bio-oil samples (Table S3); Heteroatom class distribution for whole bio-oils and derived fractions (BO, CFP_1, CFP_2, and RCFP) (Figure S3); Elemental composition of the pyrolysis bio-oils (Table S4); Van Krevelen diagrams for whole bio-oil samples and combined fractions. The data indicates that fractionation increases the compositional range coverage by FT-ICR MS (Figure S4) (PDF)

■ AUTHOR INFORMATION

Corresponding Authors

Brice Bouyssiere − *Université de Pau et des Pays de l'Adour, E2S UPPA, CNRS, IPREM, Pau 64053, France; International Joint Laboratory iC2MC: Complex Matrices Molecular Characterization, Total Research & Technology, Gonfreville, 76700 Harfleur, France;* orcid.org/0000-0001-5878-6067; Email: brice.bouyssiere@univ-pau.fr

Martha L. Chacón-Patiño − *International Joint Laboratory iC2MC: Complex Matrices Molecular Characterization, Total Research & Technology, Gonfreville, 76700 Harfleur, France; Ion Cyclotron Resonance Program, National High Magnetic Field Laboratory and Future Fuels Institute, Florida State University, Tallahassee, Florida 32310, United States;* orcid.org/0000-0002-7273-5343; Email: chacon@magnet.fsu.edu

Authors

Wladimir Ruiz − *Université de Pau et des Pays de l'Adour, E2S UPPA, CNRS, IPREM, Pau 64053, France; TotalEnergies One Tech, TotalEnergies Research & Technology Gonfreville, F-76700 Harfleur, France; International Joint Laboratory iC2MC: Complex Matrices Molecular Characterization, Total Research & Technology, Gonfreville, 76700 Harfleur, France*

German Gascon − *Université de Pau et des Pays de l'Adour, E2S UPPA, CNRS, IPREM, Pau 64053, France; International Joint Laboratory iC2MC: Complex Matrices Molecular Characterization, Total Research & Technology, Gonfreville, 76700 Harfleur, France*

Ryan P. Rodgers − *Université de Pau et des Pays de l'Adour, E2S UPPA, CNRS, IPREM, Pau 64053, France; International Joint Laboratory iC2MC: Complex Matrices Molecular Characterization, Total Research & Technology, Gonfreville, 76700 Harfleur, France; Ion Cyclotron Resonance Program, National High Magnetic Field Laboratory and Future Fuels Institute, Florida State University, Tallahassee, Florida 32310, United States;* orcid.org/0000-0003-1302-2850

David C. Dayton − *RTI International, Research Triangle Park, North Carolina 27709, United States;* orcid.org/0000-0003-3244-3722

Caroline Barrère-Mangote − *TotalEnergies One Tech, TotalEnergies Research & Technology Gonfreville, F-76700 Harfleur, France; International Joint Laboratory iC2MC: Complex Matrices Molecular Characterization, Total Research & Technology, Gonfreville, 76700 Harfleur, France*

Pierre Giusti − *TotalEnergies One Tech, TotalEnergies Research & Technology Gonfreville, F-76700 Harfleur, France; International Joint Laboratory iC2MC: Complex Matrices Molecular Characterization, Total Research & Technology, Gonfreville, 76700 Harfleur, France;* orcid.org/0000-0002-9569-3158

Complete contact information is available at: https://pubs.acs.org/10.1021/acs.energyfuels.4c02496

Author Contributions

The manuscript was written through contributions of all authors. All authors have given approval to the final version of the manuscript.

Notes

The authors declare no competing financial interest.

■ ACKNOWLEDGMENTS

Part of this work was performed at The National MagLab, funded by the National Science Foundation (DMR-2128556) and the State of Florida.

■ REFERENCES

(1) Xiu, S.; Shahbazi, A. Bio-Oil Production and Upgrading Research: A Review. *Renewable Sustainable Energy Rev.* **2012**, *16* (7), 4406−4414.

(2) Bridgwater, A. V.; Peacocke, G. V. C. Fast Pyrolysis Processes for Biomass. *Renewable Sustainable Energy Rev.* **2000**, *4* (1), 1−73.

(3) Staš, M.; Chudoba, J.; Kubička, D.; Blažek, J.; Pospíšil, M. Petroleomic Characterization of Pyrolysis Bio-Oils: A Review. *Energy Fuels* **2017**, *31* (10), 10283−10299.

(4) Staš, M.; Auersvald, M.; Kejla, L.; Vrtiška, D.; Kroufek, J.; Kubička, D. Quantitative Analysis of Pyrolysis Bio-Oils: A Review. *TrAC Trends Anal. Chem.* **2020**, *126*, No. 115857.

(5) Mohan, D.; Pittman, C. U.; Steele, P. H. Pyrolysis of Wood/Biomass for Bio-Oil: A Critical Review. *Energy Fuels* **2006**, *20*, 848−889.

(6) Chacón-Patiño, M. L.; Rowland, S. M.; Rodgers, R. P. Advances in Asphaltene Petroleomics. Part 1: Asphaltenes Are Composed of Abundant Island and Archipelago Structural Motifs. *Energy Fuels* **2017**, *31* (12), 13509−13518.

(7) Chacón-Patiño, M. L.; Rowland, S. M.; Rodgers, R. P. Advances in Asphaltene Petroleomics. Part 2: Selective Separation Method That Reveals Fractions Enriched in Island and Archipelago Structural Motifs by Mass Spectrometry. *Energy Fuels* **2018**, *32* (1), 314−328.

(8) Rodgers, R. P.; Mapolelo, M. M.; Robbins, W. K.; Chacón-Patiño, M. L.; Putman, J. C.; Niles, S. F.; Rowland, S. M.; Marshall, A. G. Combating Selective Ionization in the High Resolution Mass Spectral Characterization of Complex Mixtures. *Faraday Discuss.* **2019**, *218*, 29−51.

(9) Marhaba, T. F.; Pu, Y.; Bengraine, K. Modified Dissolved Organic Matter Fractionation Technique for Natural Water. *J. Hazard. Mater.* **2003**, *101* (1), 43−53.
(10) Sipilä, K.; Kuoppala, E.; Fagernäs, L.; Oasmaa, A. Characterization of Biomass-Based Flash Pyrolysis Oils. *Biomass Bioenergy* **1998**, *14* (2), 103−113.
(11) Oasmaa, A.; Kuoppala, E.; Solantausta, Y. Fast Pyrolysis of Forestry Residue. 2. Physicochemical Composition of Product Liquid. *Energy Fuels* **2003**, *17* (2), 433−443.
(12) Liu, Y.; Shi, Q.; Zhang, Y.; He, Y.; Chung, K. H.; Zhao, S.; Xu, C. Characterization of Red Pine Pyrolysis Bio-Oil by Gas Chromatography–Mass Spectrometry and Negative-Ion Electrospray Ionization Fourier Transform Ion Cyclotron Resonance Mass Spectrometry. *Energy Fuels* **2012**, *26* (7), 4532−4539.
(13) Oasmaa, A.; Kuoppala, E.; Ardiyanti, A.; Venderbosch, R. H.; Heeres, H. J. Characterization of Hydrotreated Fast Pyrolysis Liquids. *Energy Fuels* **2010**, *24* (9), 5264−5272.
(14) Lindfors, C.; Paasikallio, V.; Kuoppala, E.; Reinikainen, M.; Oasmaa, A.; Solantausta, Y. Co-Processing of Dry Bio-Oil, Catalytic Pyrolysis Oil, and Hydrotreated Bio-Oil in a Micro Activity Test Unit. *Energy Fuels* **2015**, *29* (6), 3707−3714.
(15) Cheng, T.; Han, Y.; Zhang, Y.; Xu, C. Molecular Composition of Oxygenated Compounds in Fast Pyrolysis Bio-Oil and Its Supercritical Fluid Extracts. *Fuel* **2016**, *172*, 49−57.
(16) Ware, R. L.; Rowland, S. M.; Rodgers, R. P.; Marshall, A. G. Advanced Chemical Characterization of Pyrolysis Oils from Landfill Waste, Recycled Plastics, and Forestry Residue. *Energy Fuels* **2017**, *31* (8), 8210−8216.
(17) Dubuis, A.; Le Masle, A.; Chahen, L.; Destandau, E.; Charon, N. Off-Line Comprehensive Size Exclusion Chromatography x Reversed-Phase Liquid Chromatography Coupled to High Resolution Mass Spectrometry for the Analysis of Lignocellulosic Biomass Products. *J. Chromatogr. A* **2020**, *1609*, No. 460505.
(18) Hertzog, J.; Garnier, C.; Mase, C.; Mariette, S.; Serve, O.; Hubert-Roux, M.; Afonso, C.; Giusti, P.; Barrere-Mangote, C. Fractionation by Flash Chromatography and Molecular Characterization of Bio-Oil by Ultra-High-Resolution Mass Spectrometry and NMR Spectroscopy. *J. Anal. Appl. Pyrolysis* **2022**, *166*, 105611.
(19) Dubuis, A.; Le Masle, A.; Chahen, L.; Destandau, E.; Charon, N. Centrifugal Partition Chromatography as a Fractionation Tool for the Analysis of Lignocellulosic Biomass Products by Liquid Chromatography Coupled to Mass Spectrometry. *J. Chromatogr. A* **2019**, *1597*, 159−166.
(20) Van Aelst, K.; Van Sinay, E.; Vangeel, T.; Cooreman, E.; Van den Bossche, G.; Renders, T.; Van Aelst, J.; Van den Bosch, S.; Sels, B. F. Reductive Catalytic Fractionation of Pine Wood: Elucidating and Quantifying the Molecular Structures in the Lignin Oil. *Chem. Sci.* **2020**, *11* (42), 11498−11508.
(21) Ruiz, W.; Gascon, G.; Chacón-Patiño, M. L.; Rodgers, R. P.; Dayton, D. C.; Barrère-Mangote, C.; Giusti, P.; Bouyssiere, B. Ultrasound-Assisted Sequential Extraction for Lignocellulose 2 Pyrolysis Bio-Oil Fractionation. Part I: Method Development. *Energy Fuels* **2024**, DOI: 10.1021/acs.energyfuels.4c01959.
(22) Scholze, B.; Meier, D. Characterization of the Water-Insoluble Fraction from Pyrolysis Oil (Pyrolytic Lignin). Part I. PY–GC/MS, FTIR, and Functional Groups. *J. Anal. Appl. Pyrolysis* **2001**, *60* (1), 41−54.
(23) Scholze, B.; Hanser, C.; Meier, D. Characterization of the Water-Insoluble Fraction from Fast Pyrolysis Liquids (Pyrolytic Lignin): Part II. GPC, Carbonyl Goups, and 13C-NMR. *J. Anal. Appl. Pyrolysis* **2001**, *58*, 387−400.
(24) da Cunha, M. E.; Schneider, J. K.; Brasil, M. C.; Cardoso, C. A.; Monteiro, L. R.; Mendes, F. L.; Pinho, A.; Jacques, R. A.; Machado, M. E.; Freitas, L. S.; Caramão, E. B. Analysis of Fractions and Bio-Oil of Sugar Cane Straw by One-Dimensional and Two-Dimensional Gas Chromatography with Quadrupole Mass Spectrometry (GC × GC/QMS). *Microchem. J.* **2013**, *110*, 113−119.
(25) Tessarolo, N. S.; Silva, R. V. S.; Vanini, G.; Casilli, A.; Ximenes, V. L.; Mendes, F. L.; de Rezende Pinho, A.; Romão, W.; de Castro, E. V. R.; Kaiser, C. R.; et al. Characterization of Thermal and Catalytic Pyrolysis Bio-Oils by High-Resolution Techniques: 1H NMR, GC$ \times$ GC-TOFMS and FT-ICR MS. *J. Anal. Appl. Pyrolysis* **2016**, *117*, 257−267.
(26) Figueirêdo, M.; Venderbosch, R. H.; Heeres, H. J.; Deuss, P. J. In-Depth Structural Characterization of the Lignin Fraction of a Pine-Derived Pyrolysis Oil. *J. Anal. Appl. Pyrolysis* **2020**, *149*, No. 104837.
(27) Harman-Ware, A. E.; Ferrell, J. R., III Methods and Challenges in the Determination of Molecular Weight Metrics of Bio-Oils. *Energy Fuels* **2018**, *32* (9), 8905−8920.
(28) Harman-Ware, A. E.; Orton, K.; Deng, C.; Kenrick, S.; Carpenter, D.; Ferrell, J. R. Molecular Weight Distribution of Raw and Catalytic Fast Pyrolysis Oils: Comparison of Analytical Methodologies. *RSC Adv.* **2020**, *10* (7), 3789−3795.
(29) Ruiz, W.; Moulian, R.; Rodgers, R. P.; Giusti, P.; Bouyssiere, B.; Marshall, A. G.; Barrère-Mangote, C.; Guillemant, J. Past to Future: Application of Gel Permeation Chromatography from Petroleomics and Metallopetroleomics to New Energies Applications: A Minireview. *Energy Fuels* **2023**, *37* (13), 8867−8882.
(30) Chacón-Patiño, M. L.; Mase, C.; Maillard, J. F.; Barrère-Mangote, C.; Dayton, D. C.; Afonso, C.; Giusti, P.; Rodgers, R. P. Petroleomics Approach to Investigate the Composition of Upgrading Products from Pyrolysis Bio-Oils as Determined by High-Field FT-ICR MS. *Energy Fuels* **2023**, *37* (21), 16612−16628.
(31) Wang, K.; Dayton, D. C.; Peters, J. E.; Mante, O. D. Reactive Catalytic Fast Pyrolysis of Biomass to Produce High-Quality Bio-Crude. *Green Chem.* **2017**, *19* (14), 3243−3251.
(32) Dayton, D. C.; Mante, O. D.; Weiner, J. Effect of Temperature on the Pilot-Scale Catalytic Pyrolysis of Loblolly Pine. *Energy Fuels* **2021**, *35* (16), 13181−13190.
(33) Smith, D. F.; Podgorski, D. C.; Rodgers, R. P.; Blakney, G. T.; Hendrickson, C. L. 21 T FT-ICR Mass Spectrometer for Ultrahigh-Resolution Analysis of Complex Organic Mixtures. *Anal. Chem.* **2018**, *90* (3), 2041−2047.
(34) Chacón-Patiño, M. L.; Moulian, R.; Barrère-Mangote, C.; Putman, J. C.; Weisbrod, C. R.; Blakney, G. T.; Bouyssiere, B.; Rodgers, R. P.; Giusti, P. Compositional Trends for Total Vanadium Content and Vanadyl Porphyrins in Gel Permeation Chromatography Fractions Reveal Correlations between Asphaltene Aggregation and Ion Production Efficiency in Atmospheric Pressure Photoionization. *Energy Fuels* **2020**, *34* (12), 16158−16172.
(35) Mase, C.; Moulian, R.; Lazzari, E.; Garnier, C.; Piparo, M.; Hubert-Roux, M.; Afonso, C.; Dayton, D. C.; Barrère-Mangote, C.; Giusti, P. Comparison of Lignocellulosic-Based Biomass Pyrolysis Processes by Multi-Scale Molecular Characterization. *J. Anal. Appl. Pyrolysis* **2024**, *177*, No. 106354.
(36) McKenna, A. M.; Chacón-Patiño, M. L.; Chen, H.; Blakney, G. T.; Mentink-Vigier, F.; Young, R. B.; Ippolito, J. A.; Borch, T. Expanding the Analytical Window for Biochar Speciation: Molecular Comparison of Solvent Extraction and Water-Soluble Fractions of Biochar by FT-ICR Mass Spectrometry. *Anal. Chem.* **2021**, *93*, 15365−15372.
(37) Chacón-Patiño, M. L.; Gray, M. R.; Rüger, C.; Smith, D. F.; Glattke, T. J.; Niles, S. F.; Neumann, A.; Weisbrod, C. R.; Yen, A.; McKenna, A. M.; et al. Lessons Learned from a Decade-Long Assessment of Asphaltenes by Ultrahigh-Resolution Mass Spectrometry and Implications for Complex Mixture Analysis. *Energy Fuels* **2021**, *35* (20), 16335−16376.
(38) Glattke, T. J.; Chacón-Patiño, M. L.; Hoque, S. S.; Ennis, T. E.; Greason, S.; Marshall, A. G.; Rodgers, R. P. Complex Mixture Analysis of Emerging Contaminants Generated from Coal Tar-and Petroleum-Derived Pavement Sealants: Molecular Compositions and Correlations with Toxicity Revealed by Fourier Transform Ion Cyclotron Resonance Mass Spectrometry. *Environ. Sci. Technol.* **2022**, *56* (18), 12988−12998.